Response of diatoms distribution to global warming and potential implications: A global model study

L. Bopp,[1] O. Aumont,[2] P. Cadule,[3] S. Alvain,[1] and M. Gehlen[1]

Received 27 May 2005; revised 7 September 2005; accepted 14 September 2005; published 13 October 2005.

[1] Using a global model of ocean biogeochemistry coupled to a climate model, we explore the effect of climate change on the distribution of diatoms, a key phytoplankton functional group. Our model results suggest that climate change leads to more nutrient-depleted conditions in the surface ocean and that it favors small phytoplankton at the expense of diatoms. At $4xCO_2$, diatoms relative abundance is reduced by more than 10% at the global scale and by up to 60% in the North Atlantic and in the subantarctic Pacific. This simulated change in the ecosystem structure impacts oceanic carbon uptake by reducing the efficiency of the biological pump, thus contributing to the positive feedback between climate change and the ocean carbon cycle. However, our model simulations do not identify this biological mechanism as a first-order process in the response of ocean carbon uptake to climate change. **Citation:** Bopp, L., O. Aumont, P. Cadule, S. Alvain, and M. Gehlen (2005), Response of diatoms distribution to global warming and potential implications: A global model study, *Geophys. Res. Lett.*, *32*, L19606, doi:10.1029/2005GL023653.

1. Introduction

[2] Diatoms, single-celled algae with silica walls, are a major component of marine phytoplankton. They tend to dominate phytoplankton community when growth conditions are optimal (e.g., high nutrient concentrations). When nutrients run out, they aggregate into flocks that sink quickly out of the ocean surface layer and therefore largely contribute to global export production of organic matter. They account for 40% of the biological pump of CO_2 [*Tréguer and Pondaven*, 2000] and are key players in ocean biogeochemistry.

[3] Recent modeled estimates of how climate change may affect marine biogeochemistry and the oceanic carbon cycle suggest reduced rates of carbon uptake mainly due to surface warming, enhanced stratification and slowed thermohaline overturning. The Oceanic Biogeochemical Models (OBM) used to derive such predictions rely on simple biogeochemical parameterizations [*Sarmiento et al.*, 1998; *Maier-Reimer et al.*, 1996; *Matear and Hirst*, 1999; *Plattner et al.*, 2001; *Dufresne et al.*, 2002] or rudimentary biological (NPZD) models [*Cox et al.*, 2000]. Such models do not represent phytoplankton diversity and therefore are unable to describe potential floristic shifts and associated biogeochemical feedbacks in response to climate variability. Because of their prominent role in biogeochemical cycles, the response of diatoms to climate change may be essential to understanding future oceanic carbon cycle behavior.

[4] Using an OBM of the new generation [*Aumont et al.*, 2003], coupled to a climate model, we present here a first estimate of how diatoms respond to climate change. We also discuss how this response impacts the oceanic carbon cycle.

2. Methodology

[5] Climate-induced changes in ocean physics are estimated from the Institut Pierre Simon Laplace Coupled Model Version 4 (IPSL-CM4) [*Marti et al.*, 2005]. As part of the Intergovernmental Panel on Climate Change's 4th Assessment Report (IPCC AR4) effort, the IPSL-CM4 climate model was integrated 140 years, starting from preindustrial conditions (CO_2 concentrations set at 1860 value, i.e., 286.2 ppm) and using the classical CMIP II scenario for atmospheric CO_2 concentrations (a 1% per year increase in CO_2, reaching $4xCO_2$ after 140 years). Output of this climate coupled simulation is available at the data archive center of IPCC AR4 Working Group 1 (http://www-pcmdi.llnl.gov/ipcc/about_ipcc.php).

[6] Monthly means output from the climate simulation are then used to drive an offline version of our OBM [*Aumont et al.*, 2003]. This OBM, named PISCES for Pelagic Interactions Scheme for Carbon and Ecosystem Studies, incorporates both multi-nutrient limitation (NO3, NH4, PO4, SiO3 and Fe) and a description of the plankton community structure with 4 Plankton Functional Groups (Diatoms, Nano-phytoplankton, Micro-zooplankton and Meso-zooplankton). In the model, diatoms differ from nano-phytoplankton because of (1) higher half saturation constants for nitrate and iron uptake, (2) Si-limitation, (3) different grazing patterns, (4) different sinking properties (Table 1). This OBM has been tested over different time ranges and used for different experiments [*Bopp et al.*, 2003; O. Aumont and L. Bopp, Globalizing results from ocean in situ iron fertilization studies, submitted to *Global and Biogeochemical Cycles*, 2005].

3. Results

[7] Hereafter we present a brief validation of our model, mainly to show how the distribution of diatoms is simulated and how it compares to available global-scale observations. Data obtained from remote sensing by NASA's Sea-viewing Field-of-view Sensor (SeaWiFS) provide the means to validate the models surface distribution of chlorophyll at

[1]Laboratoire des Sciences du Climate et de l'Environnement/Institut Pierre-Simon Laplace, CEA/CNRS, Gif sur Yvette, France.
[2]Laboratoire Océan, Climat, Exploitation et Application Numérique/Institut Pierre-Simon Laplace, CNRS/IRD/UPMC, Université Pierre et Marie Curie, Paris, France.
[3]Institut Pierre-Simon Laplace, CNRS, Université Pierre et Marie Curie, Paris, France.

0094-8276/05/2005GL023653$05.00

Table 1. Major Differences in the Parameterizations of Diatoms and Nano-phytoplankton Behavior in the PISCES Code

	Half Saturation Constants			Grazing Preferences[a]		
	Nitrate	Iron	Silicic Acid	Micro-Zooplankton	Meso-Zooplankton	Sinking Speeds[b]
Diatoms	1.3 μM	0.1–0.3 nM	2–8 μM	0.4	0.4	Mostly big particles (50–200 m/day)
Nanophytoplankton	0.3 μM	0.03 nM	-	0.6	0.1	Mostly small particles (3 m/day)

[a]This number represents the grazing preferences zooplankton has for its different preys. For meso-zooplankton, the sum is not 1. because other preys than diatoms or nanophytoplankton are considered (e.g., particles of organic carbon and micro-zooplankton).

[b]Organic matter photosynthesized by both diatoms and nanophytoplankton can end up into small or big particles. But organic matter from diatoms will contribute more to big particles because of its specific trophic web.

the global scale. A novel method, PHYSAT, based on the same data (i.e., using reflectances from SeaWiFS) was developed recently [*Alvain et al.*, 2005] and provides a qualitative estimate of the distribution of some dominant phytoplankton groups. Figures 1a and 1b show the satellite-derived and simulated distributions of chlorophyll at the surface for a climatological annual mean. Globally, the simulated patterns generally match those which are observed. In particular, an explicit representation of iron limitation of phytoplankton growth in the PISCES model enables a much better simulation of chlorophyll concentrations in High Nutrient Low Chlorophyll regions (i.e., the Southern Ocean, the equatorial Pacific and the North Pacific).

[8] Figures 1c and 1d show a diatoms index, computed as the relative time in a year when diatoms bloom are detected (from PHYSAT) or simulated. Again, the simulated patterns generally match those which are observed. Around Antarctica, diatoms blooms are often detected by PHYSAT and are present in our simulation. Both PHYSAT and the model see diatoms blooming in the frontal zones of the Southern Ocean, and with lower frequency in the equatorial Pacific. Whereas diatoms are also detected by PHYSAT in the North Pacific and Atlantic, our model over-estimates the duration of diatoms blooms in those regions.

[9] The changes in ocean physics and circulation simulated by IPSL-CM4 in response to global warming are broadly similar to previous modeling results [*Sarmiento et al.*, 2004], i.e., increased oceanic temperature (at $4xCO_2$, global average surface warming reaches +3.2°C), increased oceanic vertical stratification and decreased convective overturning (at $4xCO_2$, NADW is reduced by almost 50%), decreased arctic sea-ice cover (at $4xCO_2$, a decrease by more than 30%). The global warming experiment we performed with PISCES using those physical forcing fields shows a large decrease in primary productivity from 44 PgC/yr at $1xCO_2$ to 38.5 PgC/yr at $4xCO_2$ (Figure 2b). Increased vertical stratification of the surface ocean simulated in response to global warming leads to a large decrease in the nutrient supply to the surface ocean but to a longer growing season at high latitudes. Subsequent higher productivity at high latitudes is more than counter-balanced by an increase in the severity and the spatial extent of the oligotrophic regions [*Bopp et al.*, 2001], thus leading to a mean reduction of global ocean primary productivity.

[10] In addition to previous global modeling studies which have used much simpler approaches to represent biological activity in the ocean, this model experiment shows some large modifications of the ecosystem structure with global warming. Increased vertical stratification leads

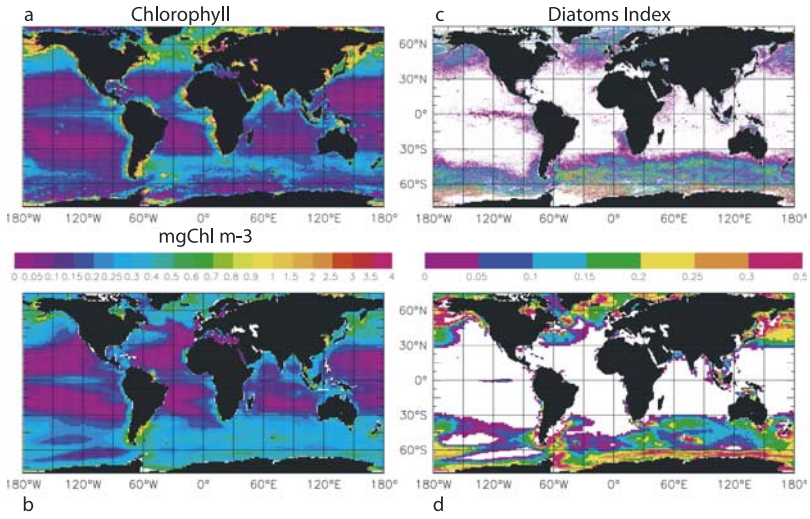

Figure 1. Satellite-derived and simulated distributions (a) and (b) of chlorophyll in mgChl m^{-3} and (c) and (d) of a diatoms index. The four panels represent climatological years, based on 1997–2003 SeaWiFs archive (Figures 1a and 1c) and on the first 10 years of our simulation (Figures 1b and 1d). The diatoms index represents the relative time in a year when diatoms are blooming, i.e., we divide the number of months when diatoms are blooming by the total number of months: PHYSAT directly diagnoses diatoms blooms [*Alvain et al.*, 2005] (Figure 1c) and diatoms blooms are diagnosed in the model when $[Chl] > 0.5$ mgChl m^{-3} and diatoms relative abundance >45% (Figure 1d).

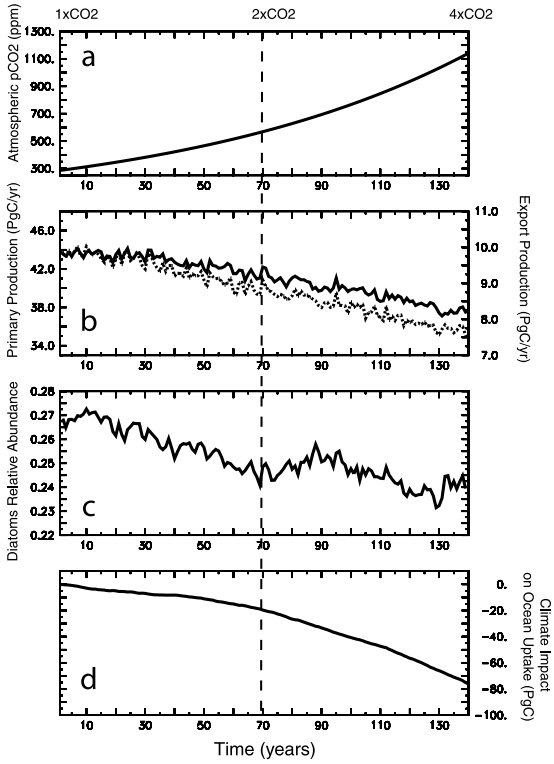

Figure 2. Time series of (a) atmospheric CO_2 (ppm) which increases at a rate of 1% y^{-1}, (b) global primary productivity (full line) in PgC y^{-1} (left axis) and global particulate export production at 100 m (dotted line) in PgC y^{-1} (right axis), (c) global mean contribution of diatoms to total chlorophyll and (d) climate change cumulative effect on oceanic carbon uptake (PgC).

to more oligotrophic conditions that are less favorable to diatoms compared to the small phytoplankton (Table 1). Indeed, PISCES simulates a decrease of diatoms relative abundance (Figures 2c, 3, and 4). Globally, the contribution of diatoms to the total chlorophyll decreases from 0.27 at $1xCO_2$ to 0.24 at $4xCO_2$ (Figure 2c). Regionally, this decrease is more pronounced in the North Atlantic, in the North Pacific and in the subantarctic Ocean, where it exceeds 0.2 (a 60% drop in diatoms relative abundance) (Figure 3).

[11] A closer look at the mechanisms that may explain diatoms retreat reveals a large correlation between nutrients diminution and diatoms retreat (Figures 4a and 4c). To gain more insight into how nutrient decrease affects diatoms relative abundance, we have plotted the changes in the nutrient limitation term of diatoms growth (Figure 4b), computed in the model to determine diatoms growth and defined as follows,

$$L_{lim} = \min\left(L_{po4}, L_{Fe}, L_{no3} + L_{nh4}, L_{Si}\right) \quad (1)$$

with,

$$L_{po4} = \frac{PO_4}{K_{po4} + PO_4} \quad (2)$$

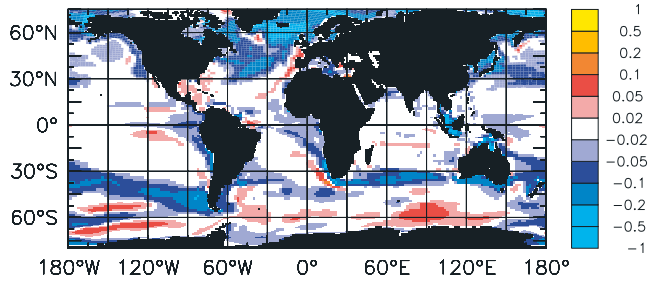

Figure 3. Simulated changes ($4xCO_2$ − $1xCO_2$) in the relative abundance of diatoms.

$$L_{fe} = \frac{Fe}{K_{Fe} + Fe} \quad (3)$$

$$L_{no3} = \frac{K_{nh4}NO_3}{K_{no3}K_{nh4} + K_{nh4}NO_3 + K_{no3}NH_4} \quad (4)$$

$$L_{nh4} = \frac{K_{no3}NH_4}{K_{no3}K_{nh4} + K_{nh4}NO_3 + K_{no3}NH_4} \quad (5)$$

$$L_{Si} = \frac{Si}{K_{Si} + Si}. \quad (6)$$

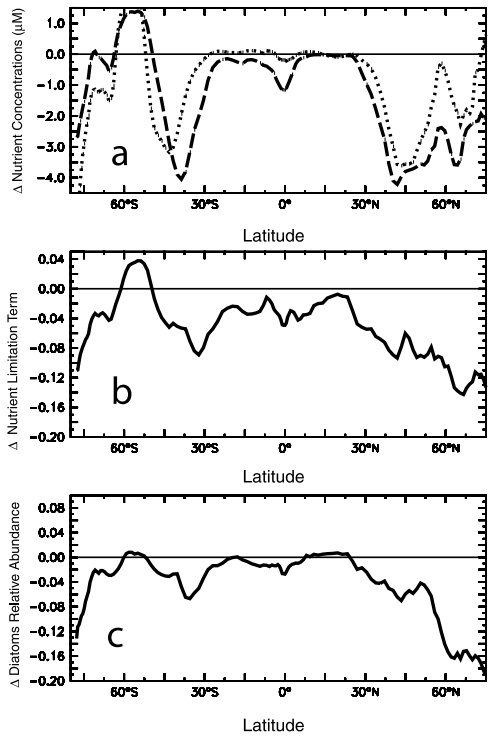

Figure 4. Zonal mean response to climate change ($4xCO_2$ − $1xCO_2$) of (a) surface concentrations of nitrate (dashed line) and silicic acid (dotted line) in μM, (b) nutrient limitation term of diatoms growth, L_{lim}, see definition in the text, and (c) the relative abundance of diatoms.

[12] L_{lim} decreases the most in the northern oceans (north of 30°N) but also between 30°S and 40°S and south of 60°S (Figure 4b). Those are typically the places where diatoms relative abundance is the most affected. A closer examination of why L_{lim} is modified reveals that Fe decrease is responsible for diatoms retreat south of 60°S, NO3 and Si decreases are responsible for diatoms retreat between 30°S and 40°S, and that NO3 decrease is responsible for diatoms retreat in the North Atlantic.

4. Discussion and Conclusion

[13] Recent modeled estimates of how climate change affect the oceanic carbon cycle have shown reduced rates of carbon uptake with global warming [*Dufresne et al.*, 2002; *Cox et al.*, 2000; *Joos et al.*, 1999; *Sarmiento et al.*, 1998; *Maier-Reimer et al.*, 1996]. The two major effects identified by those studies are a solubility effect (due to warming) and a dynamical effect (due to increased stratification that reduces anthropogenic carbon penetration). In those previous studies, changes (negative or positive) in the carbon exported by the biological pump were more or less compensated by opposite changes in the inorganic carbon transported back to the ocean surface layers by vertical mixing.

[14] Here we report on a new mechanism that involves changes in the biological pump and that may impact air-sea carbon fluxes as it decouples the upward fluxes of inorganic carbon and nutrients (driving primary productivity) from the downward flux of organic carbon. Our global warming simulation shows a large decrease of the export ratio (export production divided by the primary production) with global warming, by as much as 25% at $4xCO_2$ (from 10 PgC/yr to 7.5 PgC/yr) whereas primary production decreases by only 15% (Figure 2b). This change in the export ratio is explained by the modifications the ecosystem undergoes with global warming: diatoms are replaced by small phytoplankton and recycling of nutrients and carbon in the surface ocean is increased (i.e., the export ratio decreases). This reduction in export ratio would have a net effect on atmospheric carbon uptake as the decrease in the exported organic carbon would not be anymore compensated by the decrease in the upward flux of inorganic carbon.

[15] Moreover, this decrease in the amount of carbon exported below the photic zone is accompanied by a decrease in the mean sinking speed of organic materials (at 100 m, a decrease by 10% from 7.3 m/day at $1xCO_2$ to 6.6 m/day at $4xCO_2$), also due to the simulated floristic shift as nano-phytoplankton mostly ends up in small and slow-sinking particles. Again, this effect may substantially modify the depth at which this organic material is remineralized and modify the residence time of carbon in the sub-surface and deep oceans.

[16] To estimate how these effects contribute to a reduced uptake of carbon by the ocean, we perform another 140-yr simulation with PISCES in which atmospheric CO_2 is increased at the same rate of 1% per year but forced by the dynamical outputs of a control simulation (pre-industrial climate). The net total effect of climate change on carbon uptake is diagnosed from the difference between the global warming simulation and this additional simulation. At $4xCO_2$, the integrated effect of climate change on carbon uptake corresponds to a reduction of 76 PgC (Figure 2d). The γ_o factor, defined as the ocean carbon sensitivity to climate change [*Friedlingstein et al.*, 2003], is computed to be −16 PgC/°. This is in the range of the values that all 3D coupled climate-carbon models have found so far (−14 to −30 PgC/°) [see *Friedlingstein et al.*, 2005], all using some very simple marine biological models. We conclude from this comparison that the newly identified mechanism may contribute to the positive carbon-climate feedback but seemingly only as a second order process, first order processes being the solubility and dynamical effects.

[17] **Acknowledgments.** We thank all the people at IPSL who contributed to the development of the IPSL-CM4 model and to the climate simulations used in this study. We thank P. Brockmann and the Ferret developers for help with the analysis. This work was supported by the Environment and Climate Programme of the European Community (ORFOIS contract) and the French national programme PROOF (OCEVAR contract).

References

Alvain, S., C. Moulin, Y. Dandonneau, and F.-M. Bréon (2005), Remote sensing of phytoplankton groups in case 1 waters from global SeaWiFS imagery, *Deep Sea Res., Part I*, in press.

Aumont, O., E. Maier-Reimer, S. Blain, and P. Monfray (2003), An ecosystem model of the global ocean including Fe, Si, P co-limitations, *Global Biogeochem. Cycles*, *17*(2), 1060, doi:10.1029/2001GB001745.

Bopp, L., P. Monfray, O. Aumont, J.L. Dufresne, H. LeTreut, G. Madec, L. Terray, and J. Orr (2001), Potential impact of climate change on marine export production, *Global Biogeochem. Cycles*, *15*, 81–99.

Bopp, L., K. E. Kohfeld, C. L. Quéré, and O. Aumont (2003), Dust impact on marine biota and atmospheric pCO_2 during glacial periods, *Paleoceanography*, *18*(2), 1046, doi:10.1029/2002PA000810.

Cox, P. M., R. A. Betts, C. D. Jones, S. A. Spall, and I. J. Totterdell (2000), Acceleration of global warming due to carbon-cycle feedbacks in a coupled climate model, *Nature*, *408*, 184–187.

Dufresne, J.-L., L. Fairhead, H. Le Treut, M. Berthelot, L. Bopp, P. Ciais, P. Friedlingstein, and P. Monfray (2002), On the magnitude of positive feedback between future climate change and the carbon cycle, *Geophys. Res. Lett.*, *29*(10), 1405, doi:10.1029/2001GL013777.

Friedlingstein, P., J.-L. Dufresne, P. M. Cox, and P. Rayner (2003), How positive is the feedback between climate change and the carbon cycle?, *Tellus, Ser. B*, *55*, 692–700.

Friedlingstein, P., et al. (2005), Climate-carbon cycle feedback analysis, results from the c^4mip model intercomparison, *J. Clim.*, in press.

Joos, F., G.-K. Plattner, T. F. Stocker, O. Marchal, and A. Schmittner (1999), Global warming and marine carbon cycle feedbacks on future atmospheric CO_2, *Science*, *284*, 464–467.

Maier-Reimer, E., U. Mikolajewicz, and A. Winguth (1996), Future ocean uptake of CO_2: Interaction between ocean circulation and biology, *Clim. Dyn.*, *12*, 711–721.

Marti, O., et al. (2005), The New IPSL Climate System Model: IPSL-CM4, *Notes Sci. Pole Model Climate*, *Ref. Manual*, vol. 26, Inst. Pierre-Simon Laplace, Gif sur Yvette, France.

Matear, R. J., and A. Hirst (1999), Climate change feedback on the future oceanic CO_2 uptake, *Tellus, Ser. B*, *51*, 722–733.

Plattner, G.-K., F. Joos, T. F. Stocker, and O. Marchal (2001), Feedback mechanisms and sensitivities of ocean carbon uptake under global warming, *Tellus, Ser. B*, *53*, 564–592.

Sarmiento, J. L., T. M. C. Hughes, R. J. Stouffer, and S. Manabe (1998), Simulated response of the ocean carbon cycle to anthropogenic climate warming, *Nature*, *393*, 245–249.

Sarmiento, J. L., et al. (2004), Response of ocean ecosystems to climate warming, *Global Biogeochem. Cycles*, *18*, GB3003, doi:10.1029/2003GB002134.

Tréguer, P., and P. Pondaven (2000), Global change: Silica control of carbon dioxide, *Nature*, *406*, 358–359.

S. Alvain, L. Bopp, and M. Gehlen, LSCE, Orme des Merisiers, CE Saclay, F-91191 Gif sur Yvette, France. (laurent.bopp@cea.fr)

O. Aumont, LOCEAN, Centre IRD de Bretagne, BP 70, F-29280 Plouzané, France.

P. Cadule, IPSL, Université Pierre et Marie Curie, 4 place Jussieu, F-75252 Paris Cedex 5, France.